Original Article

Institution of MECHANICAL ENGINEERS
Journal of ENGINEERING IN MEDICINE

Proc IMechE Part H:
J Engineering in Medicine
2023, Vol. 237(1) 113–123

DOI: 10.1177/09544119221137133
journals.sagepub.com/home/pih
SAGE

Experimental study of mosquito-inspired needle to minimize insertion force and tissue deformation

Sai Teja Reddy Gidde[1], Sayemul Islam[2], Albert Kim[2] and Parsaoran Hutapea[1]

Abstract

The aim of this work is to propose a mosquito-inspired (bioinspired) design of a surgical needle that can decrease the insertion force and the tissue deformation, which are the main causes of target inaccuracy during percutaneous procedures. The bioinspired needle was developed by mimicking the geometrical shapes of mosquito proboscis. Needle prototypes were manufactured and tested to determine optimized needle shapes and geometries. Needle insertion tests on a tissue-mimicking polyvinylchloride (PVC) gel were then performed to emulate the mosquito-proboscis stinging dynamics by applying vibration and insertion velocity during the insertion. An insertion test setup equipped with a sensing system was constructed to measure the insertion force and to assess the deformation of the tissue. It was discovered that using the proposed bioinspired design, the needle insertion force was decreased by 60% and the tissue deformation was reduced by 48%. This finding is significant for improving needle-based medical procedures.

Keywords

Bioinspired surgical needle, dynamic insertion, insertion force, tissue deformation, percutaneous procedures

Date received: 27 May 2022; accepted: 19 October 2022

Introduction

Surgical needles are commonly used to reach the target locations inside of the body for various medical interventions. There have been many research efforts to design innovative surgical needles to reduce insertion force and tissue deformation for procedures such as blood sampling, biopsy, and brachytherapy.[1–3] For example, a core needle biopsy technique was utilized to extract tissue samples.[4] A sample of tissue is extracted from the organ with a needle using an ultrasound-guided percutaneous approach, which is then assessed for the presence of cancerous cells by histopathological analysis or molecular profiling.[5] Needle steering is dictated by the mechanical contact between the needle and the tissue. The effectiveness of the needle insertion is typically measured by the target accuracy,[6] which is mainly affected needle geometry, speed at which the needle is inserted, and the dynamics of the insertion.[2,7–10] These parameters also significantly affect needle path deviation due to the bending of the needle and tissue deformation.[1,2] The increase in the insertion force causes the increase in tissue deformation, which in turn will instigate the needle to deviate from its path resulting in targeting error.[7,11,12] The goal of this work is to propose a bioinspired design of a surgical needle that can minimize the insertion force and the tissue deformation for lessening the targeting error and tissue damage during the needle insertion.

The insertion force can be defined as the combination of the cutting force, the friction force, and the stiffness force that are generated during needle insertion,[13] where the friction force is the dominant force. Therefore, reducing the insertion force can lower the tissue deformation.[1,11,14] Past research has shown that the parameters such as needle geometry, velocity, and insertion method play a major role in affecting the needle insertion force.[6,15,16] To study these parameters, researchers have conducted studies to develop and

[1]Department of Mechanical Engineering, Temple University, Philadelphia, PA, USA
[2]Department of Electrical and Computer Engineering, Temple University, Philadelphia, PA, USA

Corresponding author:
Parsaoran Hutapea, Department of Mechanical Engineering, Temple University, 1947 N 12th Street, Philadelphia, PA 19122-6008, USA.
Email: hutapea@temple.edu

implement nature-inspired mechanisms. Nature-inspired designs such as honeybees barb structure, wasps stinging mechanism, and mosquito maxilla structure and vibration mechanism have been shown to minimize the insertion force of a surgical needle.[15,17–21] For instance, Sahlabadi et al.[15] studied the barb design geometry inspired by honeybee and found a decrease in the insertion force using bioinspired needles compared to that of using conventional needles. Scali et al.[18] investigated the needle insertion method inspired by the wasp and found that needle deflection is decreased compared to the standard needle insertion method. Other researchers have analyzed the insertion mechanics of jagged (or barb) structures for microneedles[22–24] and found that the bioinspired structures have a significant impact during tissue insertion.[22]

There have been also some efforts to mimic the vibration of a mosquito proboscis in soft tissues to minimize the needle insertion force.[25–28] Bi and Lin,[28] investigated the vibration effect during insertion to reduce needle deflection. Li et al.[17] have concluded that the mosquito-proboscis inspired needle, where the needle and the bioinspired cannula move in the reciprocating motion so that the needle advances incrementally and can significantly reduce the tissue deformation during insertion. Researchers have found that the mosquito-inspired vibration provides an exceptional penetrating technique for reducing the insertion force.[27–32] Additionally, it has been shown in our prior study that the use of longitudinal vibration during the insertion of a honeybee-inspired needle showed that the vibration can lower the insertion force and deflection of a needle.[33] In this work, the mosquito-inspired design parameters (i.e. shape and geometry) and the effect of dynamic insertion (i.e. vibration and insertion velocity) were investigated to study their effect on the needle insertion force and the deformation of the tissue. Specifically, the dynamic insertion method employs longitudinal vibration that is continuously applied in a sinusoidal waveform.

Since studies have also concluded that that increasing the needle insertion velocity will increase the insertion force[1,11,25,34,35], two dynamic insertion parameters, insertion velocity, and frequency will be carefully considered for evaluating the proposed mosquito-inspired needle for reduction of insertion force and tissue deformation. The major contribution of this work is the study of the effect of geometrical features such as maxilla structure and thickness on the insertion force and the tissue deformation. For example, a slight variation in the barb angle could increase the frictional contact (since the surface friction increases) and results in higher insertion force. Along with these features, this study also focuses on the effect of dynamic insertion, where vibration and insertion velocity parameters were applied to study the insertion mechanics of the proposed mosquito-inspired needle.

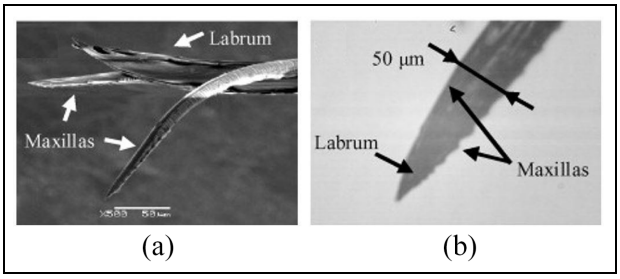

Figure 1. (a) The SEM image of the mosquito proboscis showing the elements of the maxilla, and labrum and (b) the optical image of the proboscis with a high-speed camera (magnification: 115x) ©.[36]

Materials and methods

Mosquito-inspired needle design

The design of the surgical needle in this work was inspired from mosquito proboscis. A mosquito proboscis consists of the labium, labrum, pharynx, maxilla, and mandibles.[29,30,36] The labium has a sliced tube form which allows it to open and bend away from the fascicle.[30] The other elements are the labrum (for transporting blood at the tip region), the hypopharynx (for injecting blood-thinning saliva), two maxillas (stylets with a sharp edge on the sides), and two mandibles (pointed stylets for support).[29,36] As illustrated in Figure 1(a), the two-maxilla design on each side of the labrum has a barbed structure to enable effortless needle insertion.[30] The major contribution in this work compared to our previous mosquito-inspired needle[33] study is that the geometric features of a mosquito, such as, thickness and maxilla angle were experimentally studied by changing various thickness and angle parameters. This experimental investigation of each geometrical parameter was performed to choose optimized design parameters to fundamentally understand the mechanics of mosquito-inspired needle insertion in soft tissue. It has been shown in the literature that the labrum design helps to lower the average insertion force of 18 μN during insertion in soft tissue.[30] During this penetrating process in the mosquito, the fascicle is attached on the outer layer of the skin, and it is moved forth and back within the labium at vibrating frequencies of 15[37] and 30 Hz.[31] Therefore, this vibration frequency was also considered to study its effect on the insertion force and deformation of the tissue.

The schematic representation (2D) with the geometric features of the proposed mosquito-inspired needle design in this work is shown in Figure 2(a). The proposed needle design consists of the maxilla jagged structure and labrum tip for lower insertion force.[29,30] The main goal is to reduce the insertion force, which is a combination of friction and cutting force.[13] Because of the dominant forces such as friction and cutting force acts during the needle insertion into soft tissue,[11,13–15]

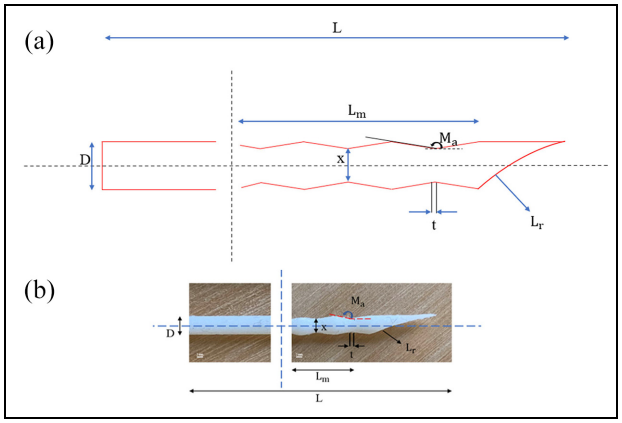

Figure 2. (a) The 2D representation of the proposed mosquito-inspired needle design consisting of the modified maxilla (a jagged structure designed for the main body of the needle) and labrum tip. (L: length of the needle, L_m: length of the maxilla, L_r: Radius of the labrum tip, M_a: Maxilla angle, t : thickness between each maxilla, x: the distance between the inner maxilla, and D: diameter of the needle); (b) 3D printed mosquito-inspired needle.

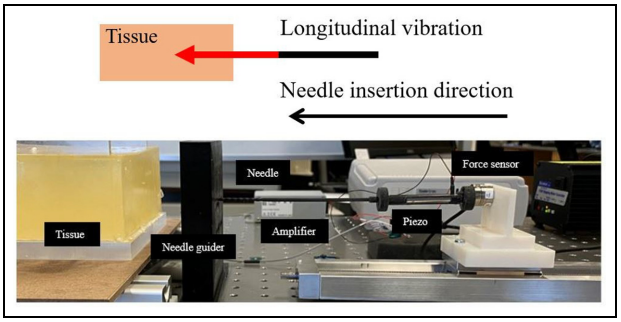

Figure 3. The applied longitudinal vibration in the insertion direction (top) and the needle insertion test setup (bottom).

the stiffness force in this work is relatively small and therefore can be neglected. It should be mentioned that the stiffness properties of the tissue mimicking material have isotropic (homogeneous) properties in order to minimize the effect of stiffness force. Reducing the friction force can be achieved by applying bioinspired shapes on the needle body and decreasing the cutting force can be achieved by adapting a bioinspired needle tip.[7] Therefore, to lessen the insertion force, the maxilla structure and labrum tip of mosquito was utilized as an inspiration to design the bioinspired needle. The symmetric maxilla structure was etched on the body of the needle with a 360° revolving shape for minimizing the friction and drag force due to the barbed structure. The labrum tip being the anchor in the needle was to decrease the deflection and to minimize the cutting force. While the reported *Aedes albopictus* mosquito fascicle diameter has 20–40 μm in diameter and 1.5–2.5 mm in length.[30] The typical medical needle for biopsy or brachytherapy procedures has 1.5–2 mm in diameter. Due to intricacy in manufacturing a true-scale needle, scaled needles were designed and manufactured up to 3 mm in diameter in this study. Past studies have shown that the needles with scaled-up diameters have shown a similar influence on the insertion force compared to the standard needles.[8,38]

The final proposed needle design parameters in this study are chosen to be $D = 3$ mm, $L = 180$ mm, $L_m = 65$ mm, $L_r = 35$ mm from outside and $t = 0.2$ mm, where D is outer diameter, L is the total length of the needle, L_m is the length of the maxilla, L_r is the radius of the labrum tip, and t is the thickness between each maxilla. In this work, the length of the jags (L_m) is 65 mm out of the total length of the needle (L = 180 mm). But to highlight the concept of jagged design along with the respective angle and thickness, they were captured closely for better understanding of the mosquito-inspired needle design parameters. The difference between L_m in Figure 2(a) and (b) is that, in Figure 2(a), the schematic representation is shown to demonstrate how a jagged structure was designed (by changing maxilla angle and thickness) and in Figure 2(b), the 3D printed mosquito-inspired needle is shown with the same design parameters.

The influential parameters such as maxilla angle and thickness were experimentally studied as their effect on the insertion force varies with the increase in angle and thickness, which is discussed in the *Results* section. The other parameter contribution is not significant in terms of its influence on the insertion force, compared to maxilla angle and thickness. Note that the higher thickness results in more gap space between each maxilla design and thus deviates the needle to bend. The bioinspired and standard needles were manufactured using the high-resolution print accuracy 3D printer (Object Connex 350, Stratasys, Inc., Eden Prairie, MN), and the 3D-manufactured needle is shown in Figure 2(b). The main purpose of designing these mosquito features on the surgical needle is that studies have shown that reducing the friction between the needle and tissue helps to steer the needle with less insertion force.[1,2,13] Furthermore, it was conjectured that the same influence of vibration could be seen on the typical needle.[25] To apply the vibration to the mosquito-inspired needle during insertion into tissue, the needle was fixed to the actuator, so that the needle can be vibrated in the longitudinal direction. Also, different frequency ranging from 0 to 500 Hz were applied to determine the desired vibrational frequency.

Test method for needle insertion

The needle insertion experimental setup, as shown in Figure 3, includes a horizontal linear stage equipped with a six-axis Force/Torque Transducer Nano17® (ATI Industrial Automation, Apex, NC) that is attached at the support. A data acquisition system using a programmable LabVIEW (National Instruments Corporation, Austin, TX) was used to

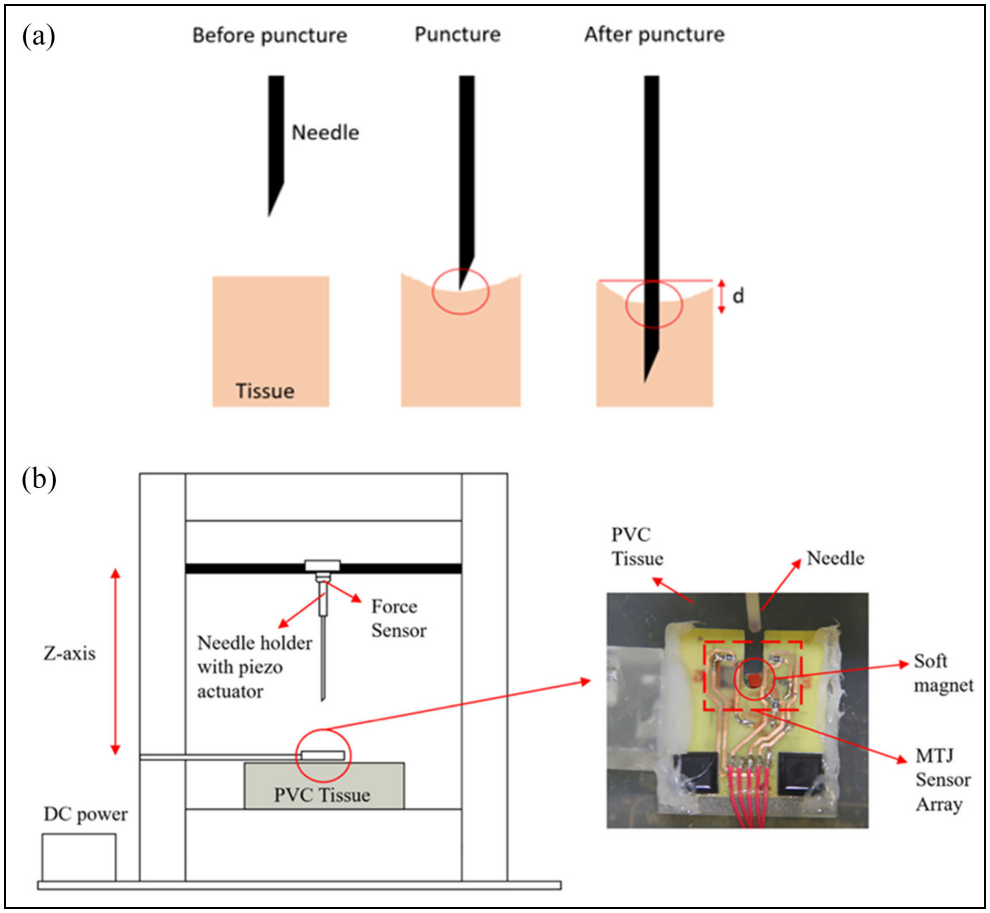

Figure 4. (a) The schematic representation of the tissue deformation from three stages (before puncture, puncture, and after puncture) defined in distance and (b) the tissue deformation test setup that mainly consists of a soft magnet (in red color) and Magnetic Tunneling Junction (MTJ) sensor.

measure the insertion force. Additionally, a piezoelectric linear actuator (Physik Instrumente, Auburn, MA) made of piezo material and an amplifier (Physik Instrumente, Auburn, MA) were utilized to vibrate the needle in the longitudinal direction with a sinusoidal waveform. The tests were conducted with mosquito-inspired needles and standard bevel-tip needles. The needle guider was used during the insertion of both the needles, so that the buckling of the needle is minimized. The insertion tests were performed in PVC tissue gel phantoms with Young's modulus of 6 kPa, which are commonly employed to mimic biological soft tissues.[9,39]

Magnetic-based tissue deformation sensing system

A tissue deformation method with magnetic sensing was used to investigate the deformation during needle insertion in tissue due to mosquito-inspired needles with vibration (Figure 4).[40] This magnetic sensing system measures tissue deformation by interpreting the magnetic field change induced by an implantable soft magnet. This soft magnet moves during needle insertion and the movement of the magnet gives the change in deformation. The schematic representation of the deformation in three stages (before puncture, puncture, and after puncture) is shown in Figure 4(a)). The sensing system test setup includes a soft magnet, magnetic field arrays, and a high-speed camera (60 fps, EOS 60D, Canon). The soft magnet was made of iron oxide (Fe_2O_3) nanoparticles embedded in silicone elastomer that should be mechanically compatible to the elastic properties of the soft tissue.[40] The soft magnets with a diameter of 3 mm and thickness of 2 mm (Figure 4) were manufactured and were positioned about 2 mm away from the needle insertion location. A total of three extremely sensitive magnetic field sensors (Micro Magnetics STJ-240) with an array were placed on a fixture and above the soft magnet.[40] A camera was used to record the tissue deformation during the insertion, which was then calibrated using the sensing data. The magnetic field strength reduces during the needle insertion (which is resulting in the deformation of the tissue) by inverse cube law[41] with a sensitivity of 0.12 Ω/μT.

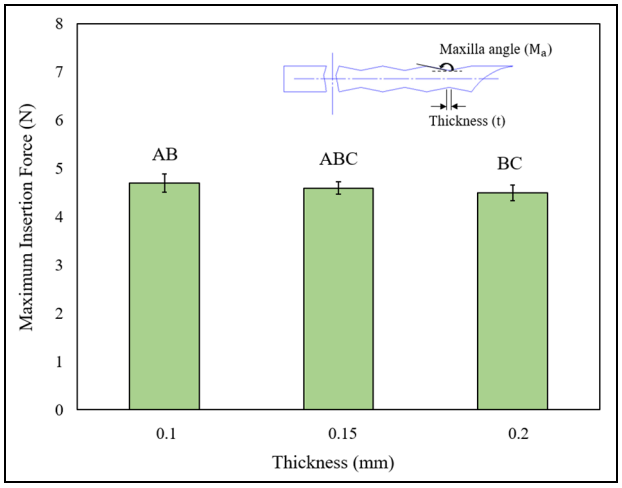

Figure 5. Effect of the thickness (t) on the maximum insertion force. The experiments were conducted without vibration and with an insertion velocity of 1 mm/s. Bars sharing the same letters are not significant (95% confidence level) and are denoted with the letters AB, ABC, and BC based on post-hoc Tukey tests.

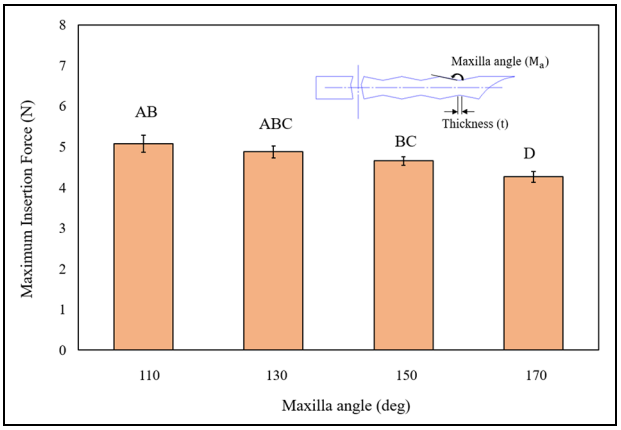

Figure 6. Effect of maxilla angles (M_a) on the maximum insertion force. The experiments were conducted without vibration and with an insertion velocity of 1 mm/s. Bars sharing the same letters are not significant and bars sharing different letters indicate the significance at the 95% confidence level based on post-hoc Tukey tests.

When the magnetic field changes, they directly correspond to the deformation of the tissue during the insertion.

Statistical analysis

The experimental data were statistically analyzed to compare the significance between the distinct groups using one-way Analysis of Variance (ANOVA) and post-hoc Tukey tests. The number of experiments conducted was three using each needle prototype and the significance of the data was analyzed using ANOVA. For the insertion force of a mosquito-inspired needle, multiple comparisons were made within the independent variables to determine the level of significance in parameters such as maxilla angle, thickness, vibration, and insertion velocity. The level of significance was set at a 95% confidence interval. The post-hoc Tukey tests reveal the significant difference between the groups. The significant factor was labeled as A, B, C, and D in plots to show the significance of the data. The same letters on the bar graph represent the non-significance and the independent letters represent the significant factor at the 95% confidence level.

Results

The insertion tests into tissue-mimicking PVC tissue gel phantoms were carried out to study the mechanics of mosquito-inspired needle insertion in tissue. First, the effect of geometrical features on the insertion force was analyzed to determine the optimized needle shapes. Next, using the optimized shapes, the influence of dynamic insertion, that is, vibration, and speed of the needle, on the insertion force was evaluated. Finally, the tissue deformation was examined using a magnetic-based sensing system to comprehend the performance of mosquito-inspired needles in terms of reducing tissue deformation.

Effect of needle geometry on insertion force

The thickness (t) and maxilla angle (M_a) (Figure 2) on the insertion force of the bioinspired needle must be first understood to determine the best needle geometries. As shown in the illustration in Figure 5, the thickness was varied but the radius of the labrum-tip (L_r = 35 mm) and the distance between inner maxillas (x = 2.20 mm) were kept constant. The value "x" depends on the maxilla angle and the labrum tip radius is also kept constant at 35 mm. Figure 5 shows the average of three maximum insertion forces for needles with different thickness (t = 0.1, 0.15, and 0.2 mm). It was noticed that the maximum insertion force of the mosquito needle decreased with an increase in thickness. Using ANOVA and post-hoc Tukey tests, it is shown that the effect of different thickness on the insertion force was not significant because of the small thickness difference. This significance in Figure 5 is denoted by A, B, and C to show the parameter difference between each value. The terms AB and ABC between 0.1 and 0.15 mm thickness and ABC and BC between 0.15 and 0.2 mm thickness indicate that the effect of thickness on the insertion force is not significant. Therefore, for this study, the final thickness of 0.2 mm was chosen based on the lowest insertion force recorded, which was a 17% force reduction.

Using a thickness of 0.2 mm, the effect of maxilla angles (M_a = 110°, 130°, 150°, and 170°) on the maximum insertion forces can be observed in Figure 6. The lower maximum insertion force was seen with the increase in the maxilla angle. This is due to removal of

Table 1. The mosquito-inspired needle geometry features the average maximum insertion force and its resulting standard deviation values.

Needle parameters	Mosquito geometry features		Average maximum insertion force (N)	Standard deviation (SD) values	Standard deviation (SD) range
Needle length (L) – 180 mm	Thickness (in mm)	0.1	4.70	0.19	$0.13 \leqslant SD \leqslant 0.19$
		0.15	4.58	0.13	
		0.2	4.50	0.16	
Needle diameter (D) – 3 mm	Maxilla angle (in deg)	110	5.08	0.21	$0.11 \leqslant SD \leqslant 0.21$
		130	4.88	0.15	
		150	4.65	0.11	
		170	4.26	0.13	

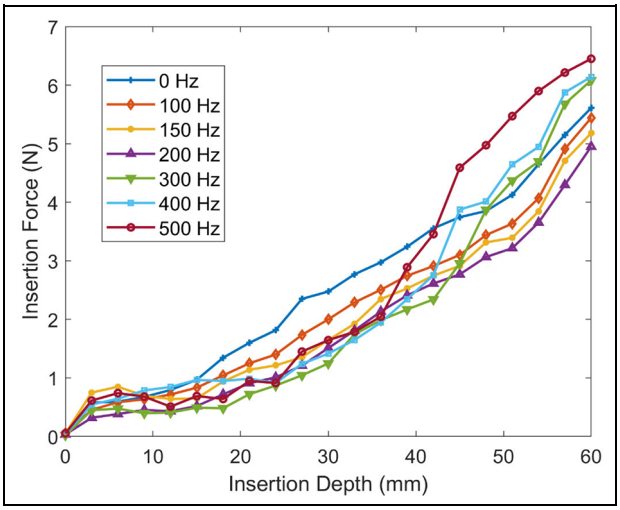

Figure 7. The vibration effect on the mosquito-inspire needle insertion force. The experiments were performed with a constant amplitude of 5 μm and at a constant insertion velocity of 1 mm/s. The standard deviation (SD) for the vibration frequency ranges from $0.05 \leqslant SD \leqslant 0.13$.

extra material on the needle body that results in less friction during insertion. Using ANOVA and post-hoc Tukey tests, the terms AB on maxilla angle 110° and ABC on maxilla angle 130° showed that the effect of maxilla angle on the insertion force is negligible. However, as the angle increases, the effect of the angle becomes more significant because of the change in the higher angle. The terms BC on maxilla angle 150° and D on maxilla angle 170° showed that the effect of maxilla angle on the insertion force of mosquito-inspired needle is significant. Therefore, for this work, the maxilla angle of 170° of maxilla angle was chosen based on the lowest insertion force recorded, which was a 9% force reduction.

The mosquito-inspired needle design parameters such as thickness (t) and maxilla angle (M_a) and their effect on the maximum insertion are shown in Table 1. Moreover, the standard deviation values are also calculated from three experimental trials. As the needle geometry is the focus of this study, the needle insertion experiments in the PVC tissue were experimentally proven to show their effect on the insertion force. Many studies in the past have also shown that average of three experiments for the needle geometry could be significant in terms of determining the insertion force.[8,38]

Effect of vibration on insertion force

Next, the effect of needle vibration on the insertion force was evaluated. The needle geometrical parameters obtained from Section 3.1 were used to fabricate the needles. The insertion tests were performed in the tissue-mimicking PVC gel with Young's Modulus (E) of 6 kPa. The vibrational frequencies varied from 0 to 500 Hz, but a constant amplitude of 5 μm, a constant insertion velocity of 1 mm/sec, and an insertion depth of 60 mm were kept constant. The average of three insertion test data was presented in Figure 7. Interestingly, from 0 to 200 Hz, the insertion force decreased with a frequency increase, but the insertion force become unpredictable above 300 Hz. It was also noticed that the slopes of the mosquito-inspired insertion forces were in general similar at 0–200 Hz frequencies. However, it was observed at higher frequencies from 300 Hz to the vibration frequency of 500 Hz, the slopes of the insertion forces changed dramatically after around 30 mm insertion depth.

Effect of insertion velocity on insertion force

The effect of insertion velocity on the insertion force can be evaluated in Figure 8. The insertion force increased with increasing velocity from 1 to 10 mm/s. The slopes of the force curves were linear which could be due to the homogenous properties of the PVC tissue phantom. The increase in force at higher insertion velocity was conjectured to be due to the increase in energy rate and/or decrease in fracture toughness[42] and viscoelastic behavior.[1] In short, it was observed from Figure 8 that the insertion velocity of 1 mm/sec provided the least insertion force.

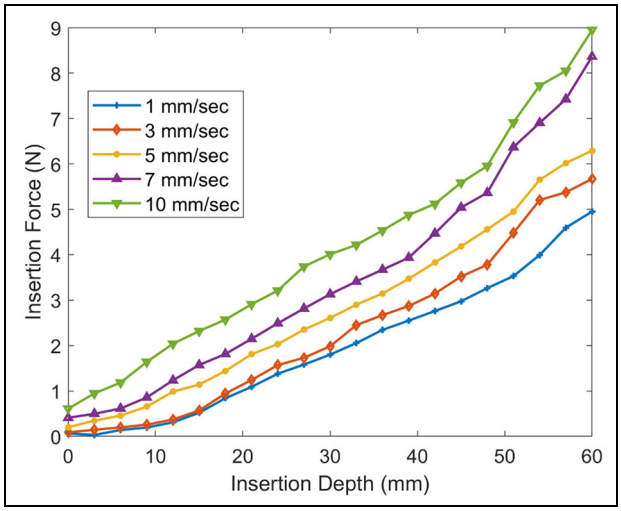

Figure 8. The insertion velocities on insertion force. The experiments were performed with a vibration of 200 Hz and an amplitude of 5 μm. The standard deviation values for the insertion velocity range from $0.05 \leqslant SD \leqslant 0.14$.

Insertion force of mosquito-inspired needle

The optimized parameters obtained in Sections 3.1–3.3 were utilized to evaluate the insertion and extraction forces of mosquito-inspired needles. The needle was inserted into tissue-mimicking PVC gels at a constant insertion velocity of 1 mm/sec and a vibrational frequency of 200 Hz with an amplitude of 5 μm. Using the average of three insertion tests, the insertion and extraction forces of the mosquito-inspired and standard needles are compared in Figure 9. It was observed that the forces of mosquito-inspired needles are lower compared to those of standard needles. It was also found that the largest insertion force of mosquito-inspired needles was 3.25 ± 0.06 N, while the largest for the standard needle was 8.10 ± 0.06 N, which shows about 60% force reduction.

Tissue deformation of mosquito-inspired needle

It has been demonstrated that the mosquito-inspired needle can decrease the insertion force. It is expected that the decrease in insertion force would result in lower tissue deformation.[7,43] The tissue deformation was evaluated using a deformation magnetic sensing system.[41] The magnetic field change indicates that the position of the magnet changed, which means the tissue is deformed during needle insertion. The magnetic field change of the soft magnet for the mosquito-inspired needle during insertion was measured to be 7.11 μT, whereas the standard needle was measured to be 9.15 μT. The slight change in the magnetic field tells us that the deformation is less when using the mosquito-inspired needle and requires less insertion force. This magnetic field change (MTJ sensor array) when using both the needles was converted to the distance (in mm) using the inverse cube law. Figure 10(c) shows the distance versus time. As shown in Figure 10(a) and (b), the deformation of the tissue due to the standard needle is 17.5 ± 0.22 mm, while the mosquito needle with vibration decreased the deformation to 11.2 ± 0.19 mm, which is a total of 36% reduction. Finally, to confirm the overall deformation in the tissue, any deformed area from the needle insertion location was measured using ImageJ. The tissue deformation area caused by mosquito-inspired needle insertion appeared as a

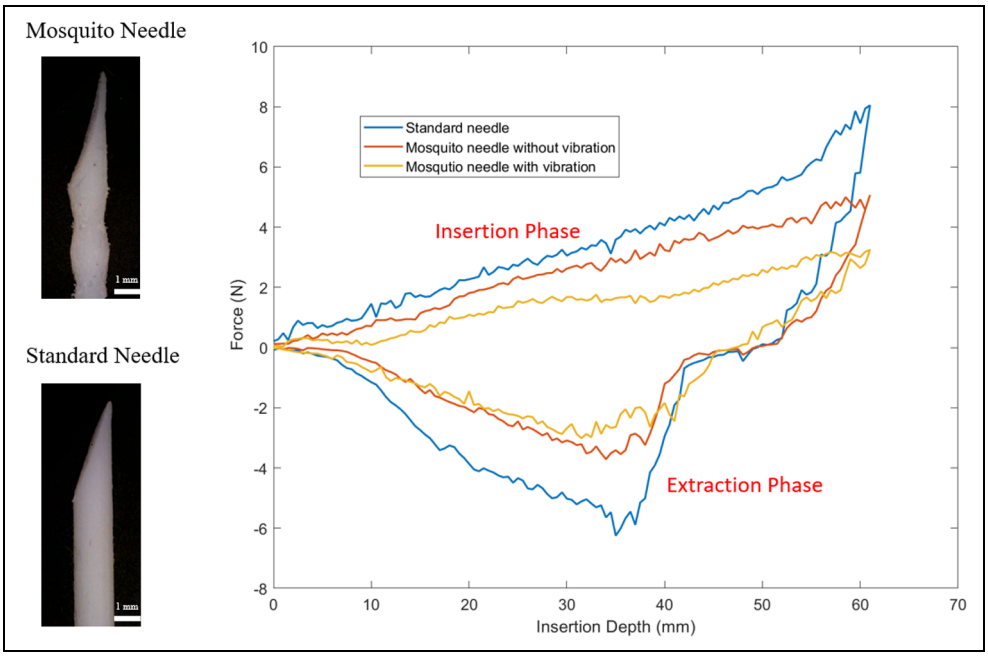

Figure 9. The insertion force profile for the mosquito-inspired and standard needles (Vibration of 200 Hz, the amplitude of 5 μm, and the insertion speed of 1 mm/s).

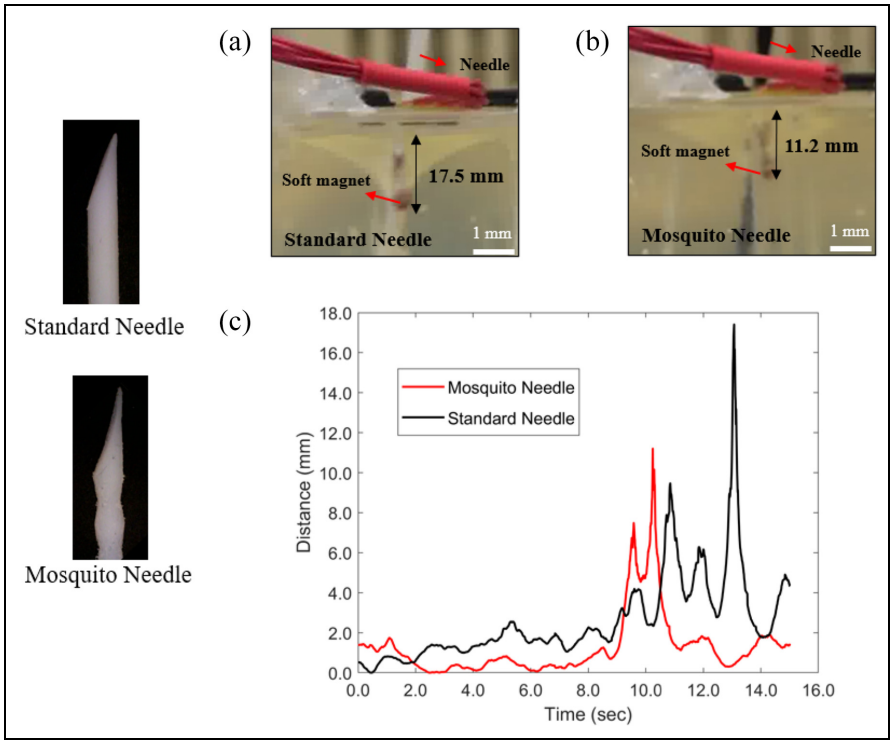

Figure 10. High speed-camera snapshots of the tissue deformation using (a) a standard needle (17.5 ± 0.22 mm) and (b) a mosquito-inspired needle (11.2 ± 0.19 mm); (c) the tissue deformation in distance (mm) as a function of time.

smaller area (0.24 mm^2) compared to the deformation area (0.46 mm^2) caused by the standard needle insertion. This study confirms that the reduction in the insertion force decreases tissue deformation.

Discussion

It is evident from the results above that the proposed mosquito-inspired needle with a dynamic insertion method can reduce the insertion force and the tissue deformation. The needle shape parameters were first determined by evaluating the maximum insertion force. The thickness (t) and maxilla angle (M_a) were varied while the distance between the maxilla (x) and L_r were kept constant. The thickness (t) of 0.2 mm and M_a of 170° were determined to be the optimized values by evaluating the maximum insertion forces as shown in Figures 5 and 6 (see Table 1 for more details). Since the bioinspired needle shape and geometry decrease the interfacial surface area between the tissue and the needle surface, the dominant friction force is decreased which contributes to the decrease in the insertion force.[13]

Next, using these parameters, the effect of dynamic insertion and the needle tip shape on the insertion force and the tissue deformation was investigated. As shown in Figure 7, from 0 to 200 Hz vibrational frequencies, the decrease in the insertion force was seen with an increase in frequencies, but the insertion force become unpredictable above 300 Hz. It was also noticed that the slopes of the insertion forces were in general similar at 0–200 Hz frequencies. However, it was observed at higher frequencies (300–500 Hz) the slopes of the insertion forces changed dramatically around 30 mm insertion depth. As mentioned previously, the insertion force is defined as the combination of cutting, friction, and stiffness forces.[13] The stiffness and cutting forces will be unaffected by the vibration, therefore only the friction force is influenced by the bioinspired needle design and the vibration.[7,42,44–48] For example, Wu et al.[48] have observed that vibration can decrease the friction force, but it does not influence the effect of tissue stiffness on the needle body. Our results show that this is true up to 200 Hz frequency but at higher frequencies and above 30 mm insertion depth, it shows a reverse trend. Increasing frequency from 300 to 500 Hz shows increasing insertion force. The results in Figure 7 follow the LuGre model prediction[49] where the friction force reaches its peak when the value of $a\omega$ (amplitude, a, times frequency, ω) is equal to the insertion velocity of the needle. In our case, the amplitude (a) was a fixed constant at 5 μm, and the frequencies varied from 100 to 500 Hz. It was understood based on the LuGre model that when $a\omega$ is less than the insertion velocity of 1 mm/s (below 200 Hz), the friction decreases compared with the non-vibration state, and the friction increases with the increase of $a\omega$ (above 300 Hz).

Additionally, the tissue viscoelastic material behavior may play a key role in influencing the steep increase in the insertion force,[50,51] especially after the needle reached 30 mm insertion depth (Figure 7). The tissue deformation during insertion impacts the tissue

stiffness that puts pressure on the needle body surface. Friction is the result of Coulomb friction, tissue adhesion, and tissue damping.[51] When the vibration frequency increases to 200 Hz, the pressure on the needle lowers resulting in a decrease in friction. But as the vibrational frequency continues to increase above 200 Hz, the friction starts to increase, which results in increasing insertion force. The result agrees with LuGre's model analysis of friction[49] that when the needle is vibrated at higher frequency, the friction force which is generated from needle bending inside the tissue dependent on Coulomb friction, static friction, and damping coefficients.[44,45] This friction force is characterized by the term Stribeck effect velocity,[45] which means that when a needle is vibrated longitudinally in a tissue (which has linear stiffness properties), the bending of the needle relative to the total velocity (vibration and insertion speed) increases the friction force, which results in increase in the insertion force.[47,48]

Figure 8 shows the insertion forces measured using different insertion velocities. It was confirmed that the insertion force increases with the increase in the insertion velocity. This is similar to the trend that was observed in different studies that the insertion force is directly proportional to insertion velocity.[1,7,11] It is shown in Figure 8 that the insertion force at 1 mm/s was 45% less than that at 10 mm/s. It was determined for the next experiments that 1 mm/s insertion velocity along with 200 Hz frequency was applied.

Figure 9 shows the insertion and extraction forces of standard needles and mosquito-inspired needles. By altering the geometry of the needle tip, the puncture force that acts at the needle tip can be decreased, which contribute to the decrease in the insertion force. This result agrees well with previous research.[52,53] It can be observed in Figure 9 that the mosquito-inspired design and dynamic insertion had a noticeable effect on lessening the insertion and extraction forces. As also examined previously in Figures 5 to 7, the friction force along the needle plays a critical role in the reduction of the insertion force. The mosquito-inspired needle has a smaller tissue-needle interfacial area. It has been shown in this study that the insertion force of a mosquito-inspired needle can be reduced by as much as 60% compared to that of standard needles. The result is very consistent as the standard deviation is in the range of $0.04 \leqslant \mathrm{SD} \leqslant 0.12$.

A big challenge when decreasing the diameter of a bioinspired needle prototype is the thickness of the maxilla design on the needle body. For future work, meso-scale manufacturing method can be explored for fabricating the proposed bioinspired needle prototypes. The maxilla structure can be cut out from the standard needle with a high accuracy of 0.1–5 mm. It should be pointed out that bioinspired needle size-scale study in a previous work showed that irrespective of the diameter size, the insertion force decreases significantly.[44] Although this study is limited to the use of 3D scaled printed needles, it is expected that the resulting insertion mechanics of scaled needles would be qualitatively similar with that of true-scaled needles.

The reduction in the insertion force should lead to a decrease in tissue deformation. Here, some experiments were performed using the optimized conditions discussed previously to measure the tissue deformation using a magnetic-based sensing method,[41] as shown in Figure 10. It is understandable that when a needle is moving in tissue, the needle would cause tissue deformation.[1,7,43] It can be observed in Figure 10(a) and (b), that the length (depth) of the deformation mosquito-inspired needle (11.2 mm) is about 36% less than that of the standard needle (17.5 mm). This was determined by observing the magnetic field change which was converted to the distance (length) using inverse cube law with the optically measured reference data (Figure 10(c)). As shown in Figure 10(a) and (b), the deformation areas from the insertion of mosquito-inspired needle were calculated to be 48% less than that of the standard needle. The images were taken during the needle insertion at the maximum depth. However, the deformation shown in Figure 10(b) looks like a triangular area where the area was large for a standard needle ($0.46\,mm^2$) compared to the mosquito-inspired needle ($0.24\,mm^2$). Moreover, the position of the magnet also changes due to the needle insertion, which was tracked by the sensing method. The decrease in tissue deformation indicates mosquito-inspired needle design coupled with the dynamic insertion can be used to improve the target accuracy[54,55] and potentially can be effective to reduce tissue damage in percutaneous procedures.[56] There are obviously differences between a homogenous (isotropic) PVC tissue and real tissue properties. The PVC tissue used here is isotropic, but it still has viscoelastic behavior. The properties of real tissues are anisotropic and non-linearly viscoelastic. These complex properties are very challenging to characterize and to mimic for any study due to the inherent tissue variation, that is, brain, liver, kidney, etc. The challenge in this work is the measurement of tissue deformation. In our case, since the PVC is transparent, placing the soft magnet is more convenient for deformation measurement. For future work, different types of sensors and measurement methods should be investigated for direct measurement of real tissue deformation.

Conclusions

The optimized geometric parameters of the mosquito-inspired needle were determined by studying their effect on the insertion force and the tissue deformation. The results showed that it was feasible to achieve insertion force reduction by as much as 60% using a mosquito-inspired needle. Furthermore, the effect of the mosquito-inspired needle on tissue deformation was also studied using a magnetic-based sensing system. It was concluded that there was a 36% reduction in tissue deformation as measured by the deformation depth

between the tissue surface to the needle tip. It was also observed that there was a 48% reduction in the tissue deformation area. The presented data support the hypothesis that the bioinspired needle can minimize the insertion force and tissue deformation. Future work will investigate the force behavior, the deformation of the tissue, and the tissue damage caused by the mosquito-inspired needle insertion on real tissues such as bovine brains and livers. Development of true-scale prototypes using metal needle materials is also currently ongoing. In summary, the findings in this study are very encouraging as this will help researchers to advance bioinspired needles for more efficient needle interventional procedures.

Acknowledgements

The authors would like to thank Mr. Moonchul Park for his contribution to the preparation of a soft magnet for the novel magnetic sensing system. Finally, the authors would like to acknowledge the National Science Foundation (CMMI Award #1917711) for the financial support.

Declaration of conflicting interests

The author(s) declared no potential conflicts of interest with respect to the research, authorship, and/or publication of this article.

Funding

The author(s) disclosed receipt of the following financial support for the research, authorship, and/or publication of this article: National Science Foundation CMMI Award #1917711

Ethical approval

Not required.

ORCID iD

Parsaoran Hutapea https://orcid.org/0000-0001-6917-1252

References

1. van Gerwen DJ, Dankelman J and van den Dobbelsteen JJ. Needle–tissue interaction forces – A survey of experimental data. *Med Eng Phys* 2012; 34(6): 665–680.
2. Abolhassani N, Patel R and Moallem M. Needle insertion into soft tissue: a survey. *Med Eng Phys* 2007; 29(4): 413–431.
3. Podder TK, Dicker AP, Hutapea P, et al. A novel curvilinear approach for prostate seed implantation. *Med Phys* 2012; 39(4): 1887–1892.
4. Piccinino F, Sagnelli E, Pasquale G, et al. Complications following percutaneous liver biopsy. A multicentre retrospective study on 68,276 biopsies. *J Hepatol* 1986; 2(2): 165–173.
5. Kim JW and Shin SS. Ultrasound-guided percutaneous core needle biopsy of abdominal viscera: tips to ensure safe and effective biopsy. *Korean J Radiol* 2017; 18(2): 309–322.
6. DiMaio SP and Salcudean SE. Needle insertion modeling and simulation. *IEEE Trans Robot Autom* 2003; 19(5): 864–875.
7. Yang C, Xie Y, Liu S, et al. Force modeling, identification, and feedback control of robot-assisted needle insertion: a survey of the literature. *Sensors* 2018; 18(2): 561.
8. Jiang S, Li P, Yu Y, et al. Experimental study of needle-tissue interaction forces: effect of needle geometries, insertion methods, and tissue characteristics. *J Biomech* 2014; 47(13): 3344–3353.
9. McGill CS, Schwartz JA, Moore JZ, et al. Effects of insertion speed and trocar stiffness on the accuracy of needle position for brachytherapy. *Med Phys* 2012; 39(4): 1811–1817.
10. Liang D, Jiang S, Yang Z, et al. Simulation and experiment of soft-tissue deformation in prostate brachytherapy. *Proc IMechE, Part H: J Engineering in Medicine* 2016; 230(6): 532–544.
11. Abolhassani N, Patel R and Moallem M. Control of soft tissue deformation during robotic needle insertion. *Minim Invasive Ther Allied Technol* 2006; 15(3): 165–176.
12. de Jong TL, van de Berg NJ, Tas L, et al. Needle placement errors: do we need steerable needles in interventional radiology? *Med Device* 2018; 11: 259–265.
13. Okamura AM, Simone C and O'Leary MD. Force modeling for needle insertion into soft tissue. *IEEE Trans Biomed Eng* 2004; 51(10): 1707–1716.
14. Mahvash M and Dupont PE. Fast needle insertion to minimize tissue deformation and damage. In: *IEEE international conference on robotics and automation*, 2009; pp.3097–3102. New York: IEEE.
15. Sahlabadi M, Khodaei S, Jezler K, et al. Insertion mechanics of bioinspired needles into soft tissues. *Minim Invasive Ther Allied Technol* 2018; 27(5): 284–291.
16. Begg ND and Slocum AH. Audible frequency vibration of puncture-access medical devices. *Med Eng Phys* 2014; 36(3): 371–377.
17. Li ADR, Putra KB, Chen L, et al. Mosquito proboscis-inspired needle insertion to reduce tissue deformation and organ displacement. *Sci Rep* 2020; 10(1): 12248.
18. Scali M, Kreeft D, Breedveld P, et al. Design and evaluation of a wasp-inspired steerable needle. *Proc. SPIE* 2017; 10162: 34–46.
19. Gurera D, Bhushan B and Kumar N. Lessons from mosquitoes painless piercing. *J Mech Behav Biomed Mater* 2018; 84: 178–187.
20. Shoffstall AJ, Srinivasan S, Willis M, et al. A mosquito inspired strategy to implant microprobes into the brain. *Sci Rep* 2018; 8(1): 122.
21. Scali M, Pusch TP, Breedveld P, et al. Ovipositor-inspired steerable needle: design and preliminary experimental evaluation. *Bioinspir Biomim* 2017; 13(1): 016006.
22. Kim J, Park S, Nam G, et al. Bioinspired microneedle insertion for deep and precise skin penetration with low force: why the application of mechanophysical stimuli should be considered. *J Mech Behav Biomed Mater* 2018; 78: 480–490.
23. Izumi H, Yajima T, Aoyagi S, et al. Combined harpoon-like jagged microneedles imitating mosquito's proboscis

and its insertion experiment with vibration. *IEEJ Trans Electr Electron Eng* 2008; 3(4): 425–431.
24. Davis SP, Landis BJ, Adams ZH, et al. Insertion of microneedles into skin: measurement and prediction of insertion force and needle fracture force. *J Biomech* 2004; 37(8): 1155–1163.
25. Tan L, Qin X, Zhang Q, et al. Effect of vibration frequency on biopsy needle insertion force. *Med Eng Phys* 2017; 43: 71–76.
26. Barnett AC, Jones JA, Lee YS, et al. Compliant needle vibration cutting of soft tissue. *J Manuf Sci Eng* 2016; 138(11): 1–9.
27. Huang YC, Tsai MC and Lin CH. A piezoelectric vibration-based syringe for reducing insertion force. *IOP Conf Ser Mater Sci Eng* 2012; 42(1): 012020.
28. Bi D and Lin Y. Vibrating needle insertion for trajectory optimization. In: *IEEE world congress on intelligent control and automation*, 2008; pp.7444–7448. New York: IEEE.
29. Lenau TA, Hesselberg T, Drakidis A, et al. Mosquito inspired medical needles. *Proc SPIE* 2017; 10162: 1016208.
30. Kong XQ and Wu CW. Measurement and prediction of insertion force for the mosquito fascicle penetrating into human skin. *J Bionic Eng* 2009; 6(2): 143–152.
31. Aoyagi S, Izumi H and Fukuda M. Biodegradable polymer needle with various tip angles and consideration on insertion mechanism of mosquito's proboscis. *Sens Actuators A Phys* 2008; 143(1): 20–28.
32. Gidde STR and Hutapea P. Design and experimental evaluation of mosquito-inspired needle structure in soft materials. In: *ASME international mechanical engineering congress and exposition*, 2020; 84522: 1–3. New York: ASME.
33. Gidde STR, Ciuciu A, Devaravar N, et al. Effect of vibration on insertion force and deflection of bioinspired needle in tissues. *Bioinspir Biomim* 2020; 15(5): 054001.
34. Healey AE, Evans JC, Murphy MG, et al. In vivo force during arterial interventional radiology needle puncture procedures. *Stud Health Technol Inform* 2005; 111: 178–184. https://pubmed.ncbi.nlm.nih.gov/15718723/ (accessed 24 February 2022)
35. Clement RS, Unger EL, Ocón-Grove OM, et al. Effects of axial vibration on needle insertion into the tail veins of rats and subsequent serial blood corticosterone levels. *J Am Assoc Lab Anim Sci* 2016; 55(2): 204–212.
36. Izumi H, Suzuki M, Aoyagi S, et al. Realistic imitation of mosquito's proboscis: electrochemically etched sharp and jagged needles and their cooperative inserting motion. *Sens Actuators A Phys* 2011; 165: 115–123.
37. Ramasubramanian MK, Barham OM and Swaminathan V. Mechanics of a mosquito bite with applications to microneedle design. *Bioinspir Biomim* 2008; 3(4): 046001.
38. Sahlabadi M and Hutapea P. Novel design of honeybee-inspired needles for percutaneous procedure. *Bioinspir Biomim* 2018; 13(3): 036013.
39. Li W, Belmont B and Shih A. Design and manufacture of polyvinyl chloride (PVC) tissue mimicking material for needle insertion. *Procedia Manuf* 2015; 1: 866–878.
40. Islam S, Shah V, Gidde STR, et al. A machine learning enabled wireless intracranial brain deformation sensing system. *IEEE Trans Biomed Eng* 2020; 67(12): 3521–3530.
41. Michaud A. On the magnetostatic inverse cube law and magnetic monopoles. *Int J Eng Res Dev* 2013; 7: 50–66.
42. Asadian A, Patel RV and Kermani MR. Dynamics of translational friction in needle-tissue interaction during needle insertion. *Ann Biomed Eng* 2014; 42(1): 73–85.
43. Sahlabadi M and Hutapea P. Tissue deformation and insertion force of bee-stinger inspired surgical needles. *J Med Device* 2018; 12(3): 034501.
44. Gidde STR. *Bioinspired surgical needle insertion mechanics in soft tissues for percutaneous procedures*. Ph.D. Dissertation, Temple University, US, 2021. https://www.proquest.com/docview/2572595368?pq-origsite=scholar&fromopenview=true (accessed 18 October 2021)
45. Khalaji I, Hadavand M, Asadian A, et al. Analysis of needle-tissue friction during vibration-assisted needle insertion. In: *IEEE/RSJ international conference on intelligent robots and systems*, 2013; pp.4099–4104. New York: IEEE.
46. Wang Y, Fu Z, Zhao ZF, et al. Experimental study of the optimum puncture pattern of robot-assisted needle insertion into hyperelastic materials. *Proc IMechE, Part H: J Engineering in Medicine* 2021; 235(1): 28–43.
47. Mahvash M and Dupont PE. Mechanics of dynamic needle insertion into a biological material. *IEEE Trans Biomed Eng* 2010; 57(4): 934–943.
48. Wu W, Zhou J, Huang P, et al. Antifriction mechanism of longitudinal vibration-assisted insertion in DBS. *Ann Biomed Eng* 2021; 49(9): 2057–2065.
49. Canudas-de-Wit C. Comments on "A new model for control of systems with friction". *IEEE Trans Automat Contr* 1998; 43(8): 1189–1190.
50. Leibinger A, Forte AE, Tan Z, et al. Soft tissue phantoms for realistic needle insertion: a comparative study. *Ann Biomed Eng* 2016; 44(8): 2442–2452.
51. Wu W, Xu C, Pan C, et al. Effect of vibration frequency on frictional resistance of brain tissue during vibration-assisted needle insertion. *Med Eng Phys* 2020; 86: 35–40.
52. Towler MA, McGregor W, Rodeheaver GT, et al. Influence of cutting edge configuration on surgical needle penetration forces. *Emerg Med J* 1988; 6(6): 475–481.
53. Chebolu A and Mallimoggala A. Modelling of cutting force and deflection of medical needles with different tip geometries. *Procedia Mater Sci* 2014; 5: 2023–2031.
54. Webster RJ, Memisevic J and Okamura AM. Design considerations for robotic needle steering. In: *Proceeding of the 2005 IEEE international conference on robotics and automation*. 2005; pp.3588–94. New York: IEEE. https://doi.org/10.1109/ROBOT.2005.1570666.
55. Wan G, Wei Z, Gardi L, et al. Brachytherapy needle deflection evaluation and correction. *Med Phys* 2005; 32(4): 902–909.
56. Gidde STR, Acharya SR, Kandel S, et al. Assessment of tissue damage from mosquito-inspired surgical needle. *Minim Invasive Ther Allied Technol* 2022; 31: 1112–1121.